

# Kosterlitz–Thouless transition of the quasi two-dimensional trapped Bose gas

Markus Holzmann

*LPTMC, Université Pierre et Marie Curie, 4 Place Jussieu, 75005 Paris, France; and LPMMC, CNRS-UJF, BP 166, 38042 Grenoble, France*

Werner Krauth

*CNRS-Laboratoire de Physique Statistique, Ecole Normale Supérieure, 24 rue Lhomond, 75231 Paris Cedex 05, France*

(Dated: November 1, 2018)

We present Quantum Monte Carlo calculations with up to  $N = 576\,000$  interacting bosons in a quasi two-dimensional trap geometry closely related to recent experiments with atomic gases. The density profile of the gas and the non-classical moment of inertia yield intrinsic signatures for the Kosterlitz–Thouless transition temperature  $T_{KT}$ . From the reduced one-body density matrix, we compute the condensate fraction, which is quite large for small systems. It decreases slowly with increasing system sizes, vanishing in the thermodynamic limit. We interpret our data in the framework of the local-density approximation, and point out the relevance of our results for the analysis of experiments.

PACS numbers: 05.30.Jp, 03.75.Hh

Phase transitions in two-dimensional systems with a continuous order parameter are of special interest because long-range order is absent at finite temperatures, as a consequence of the Mermin–Wagner theorem [1, 2]. Instead, a Kosterlitz–Thouless phase transition [3] can separate the high-temperature disordered phase with exponential decay of the order parameter from a low-temperature ordered phase with algebraically decaying order parameter, which was proposed by Berezinskii [4].

Recently, the Kosterlitz–Thouless phase transition was observed in trapped quasi two-dimensional Bose gases of  $^{87}\text{Rb}$  atoms [5, 6], but the interpretation of the experimental data was rendered difficult because of relatively strong interactions in two dimensions, the trap confinement, and pronounced finite-size corrections. Moreover, the ideal two-dimensional trapped Bose gas is not a good vantage point to approach the weakly interacting gas: the former Bose-condenses at finite temperature (with a diverging density in the center), whereas the latter becomes a superfluid, but with vanishing condensate fraction.

Quantum Monte Carlo (QMC) calculations allow us to compute the thermodynamic properties of interacting Bose systems [7] for a finite number  $N$  of particles, and for a wide range of microscopic interaction parameters. The calculations are practically free of systematic errors. For trapped atomic gases, very large particle numbers can be handled, in confining geometries relevant to current experiments [8, 9, 10]. The ideal Bose gas enters these calculations in an exact way, and only pair interactions give rise to the usual Metropolis rejection process [11].

In this paper, we present QMC calculations of three-dimensional trapped bosons interacting with an  $s$ -wave pseudopotential in a pancake-shaped harmonic trap with frequencies  $\omega = \omega_x = \omega_y \ll \omega_z$ . Our particle numbers range from  $N = 2000$  to  $N = 576\,000$ , the latter exceed-

ing current experiments by more than one order of magnitude. The diagonal many-particle density matrix directly yields the density profile and the non-classical moment of inertia. Both allow us to locate the phase transition. We also determine the condensate fraction explicitly from the largest eigenvalue of the reduced off-diagonal one-particle density matrix. In a trap, this calculation is more complicated than in a homogeneous system, where the  $k = 0$  groundstate wavefunction is trivially known and where the groundstate occupation governs the long-range behavior of the off-diagonal one-particle density matrix.

The trapped ideal two-dimensional Bose gas shows a Bose–Einstein transition [12] at a non-vanishing temperature  $T_{\text{BEC}}^0 = \sqrt{6N\omega^2/\pi^2}$  (we choose units with  $\hbar = m = \omega = 1$ , where  $m$  is the atomic mass). The central density diverges logarithmically with  $N$  (see Fig. 1). This implies that interaction effects play a much more pronounced role, even above the transition temperature, than in three-dimensional traps.

As in the experiment [6], we allow for a finite extension  $\omega_z$  of the trap in the  $z$ -direction, keeping the level spacing on the order of the temperature:  $\omega_z = 0.55 T_{\text{BEC}}^0$ . In the many-body density matrix, the  $z$ -dependence is dominated by a (normalized) single-particle contribution,  $\rho(z, z')$ , which separates out, and the effective two-dimensional interaction strength is given by

$$g = \frac{4\pi\hbar^2 a_0}{m} \int dz [\rho(z, z)]^2, \quad (1)$$

where  $a_0$  is the three-dimensional  $s$ -wave scattering length. For particles distributed in  $z$  according to the groundstate of the harmonic oscillator, Eq. (1) reduces to  $g = \tilde{g} \equiv a_0 \sqrt{8\pi\omega_z}$ . For our simulations, we have used the experimental value  $\tilde{g} = 0.13$  [6], however, the actual value of  $g$  can be obtained directly from the computed density profile in the  $z$ -direction.

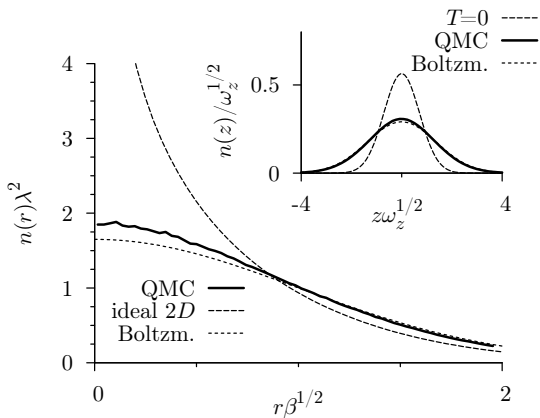


FIG. 1: Two-dimensional density profile  $n(r)\lambda^2$  at  $T = T_{\text{BEC}}^0$  for  $N = 576\,000$ , compared to the saturation density of the ideal Bose gas and the density profile of an ideal gas of distinguishable particles. The inset compares the density profile in  $z$  to the groundstate distribution of the harmonic oscillator and to the ideal gas of distinguishable particles.

We study the anisotropic trap at temperatures comparable to  $T_{\text{BEC}}^0$  where it is indeed quasi two-dimensional because the extension in  $z$  is comparable to the de-Broglie wavelength  $\lambda = \sqrt{2\pi/mT}$ . Formally, the three-dimensional Bose–Einstein transition temperature  $0.94 N^{1/3}(\omega^2\omega_z)^{1/3}$  is of the same order as  $T_{\text{BEC}}^0$ . However, the three-dimensional limit requires that  $\omega_z/\omega$  remains constant independent of the system size in contrast to our quasi two-dimensional limit where  $\omega_z/\omega \sim N^{1/2}$ .

Recent numerical calculations [13] have determined the critical density  $n_c$  at the Kosterlitz–Thouless transition in the weakly interacting two-dimensional homogeneous Bose gas of density  $n$ ,

$$n_c\lambda^2 \simeq \ln \frac{380}{mg}. \quad (2)$$

The interaction  $g$  enters this expression only logarithmically, and the differences between the actual  $g$  and  $\tilde{g}$ , of the order of 40% at  $T_{\text{KT}}$ , only results in a 6% shift in the critical density.

In the trapped Bose gas, within the local-density approximation, the transition takes place when the central density  $n(0)$  equals the critical density of the homogeneous gas, in our case  $n_c(0)\lambda^2 \simeq 8$ . Mean-field theory [14] predicts that the Kosterlitz–Thouless transition is somewhat below  $T_{\text{BEC}}^0$ :

$$\frac{T_{\text{KT}}^{\text{mf}}}{T_{\text{BEC}}^0} = \left(1 + \frac{3g}{\pi^3} [n_c(0)\lambda^2]^2\right)^{-\frac{1}{2}}. \quad (3)$$

The mean-field value of  $T_{\text{KT}}$ , together with the numerical value of Eq. (2) for the critical density in the center of the trap allows to determine the critical temperature of the Kosterlitz–Thouless transition in the trap, in our case  $T_{\text{KT}}^{\text{mf}} \simeq 0.75 T_{\text{BEC}}^0$ .

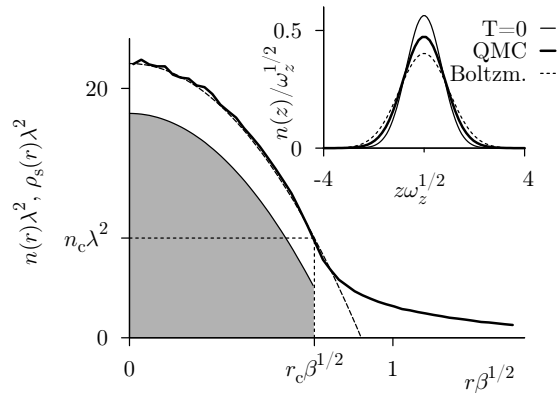


FIG. 2: Two-dimensional density profile  $n(r)\lambda^2$  at temperature  $T = 0.5 T_{\text{BEC}}^0$  for  $N = 576\,000$  (thick line), compared to the Thomas–Fermi profile of Eq. (4) (with  $g = 0.109$ , dashed line). The ansatz of Eq. (5) for the superfluid density  $\rho_s(r)$ , with the universal jump at  $r = r_c$ , corresponds to the shaded region. The inset compares the density profile in the tightly confined  $z$ -direction to the groundstate distribution of the harmonic oscillator and the distribution of an ideal gas of distinguishable particles.

In Fig. 1, we show the two-dimensional density profile  $n(r)$  with  $r = \sqrt{x^2 + y^2}$  from our QMC calculations at  $T = T_{\text{BEC}}^0$  for  $N = 576\,000$ . We also illustrate the large deviations from the saturation density of the two-dimensional ideal Bose gas [11]. Indeed, the density profile is closer to that of ideal quantum Boltzmann particles described by the density matrix of the harmonic oscillator. The density is everywhere below the critical value, confirming that the interacting gas remains in its high-temperature phase at lower temperatures than the ideal Bose gas.

In Fig. 2, we show the analogous density profile at temperature  $T/T_{\text{BEC}}^0 = 0.5$ , again for  $N = 576\,000$  particles. The central density is now well in excess of the critical value of Eq. (2). We may define a “critical radius”  $r_c$ , which separates the “inner region” of the trap, with  $r < r_c$  and  $n(r) > n_c$ , from an “outer region” with  $r > r_c$  and with  $n(r) < n_c$ . In the local-density approximation, the inner region is in the superfluid phase, whereas the outer region is normal. At the critical radius, the density is at the Kosterlitz–Thouless phase-transition temperature. In the inner region,  $n(r)$  is very well described by a Thomas–Fermi profile

$$n(r) = n(0) - \frac{\omega^2 r^2}{2g}, \quad r < r_c, \quad (4)$$

with the effective two-dimensional interaction parameter at this temperature  $g = 0.107$ , obtained, via Eq. (1), directly from the density profile in  $z$  (see the inset of Fig. 2). The latter is wider than the groundstate distribution of the harmonic oscillator, so that  $g$  is smaller than  $\tilde{g}$ . The density profile in  $r$ , whose width depends linearly on  $g^{-1}$ ,

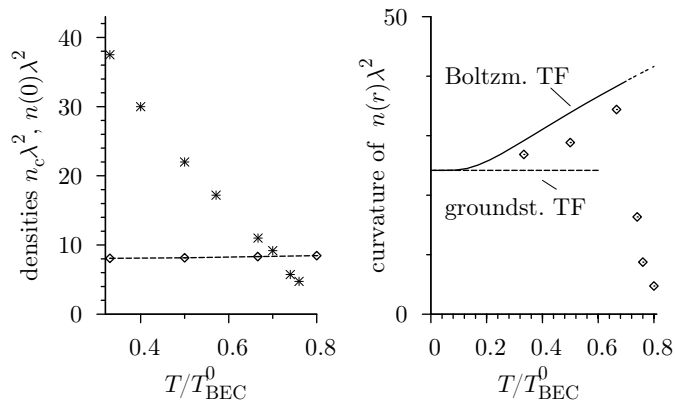


FIG. 3: *Left*: Densities  $n_c \lambda^2$  and  $n(0) \lambda^2$  vs.  $T/T_{\text{BEC}}^0$  for the quasi two-dimensional gas with  $N = 576\,000$ . The intersection of both curves leads to a transition temperature  $T_{\text{KT}} \simeq 0.70$ . *Right*: central curvature  $\kappa$  compared to the groundstate Thomas–Fermi curvature, Eq. (4), with  $g = \tilde{g}$  and with  $g$  corresponding to an ideal gas of distinguishable particles. The central curvature changes slope at  $T_{\text{KT}}$ .

is more sensitive to the detailed value of the interaction than the transition temperature, which decreases with the logarithm of  $g$ .

In Fig. 3, we plot the central density  $n(0) \lambda^2$  and also the (central) curvature  $\kappa = -(\lambda^2/\beta) \partial n(r)/\partial(r^2)|_{r=0}$ . The curvature of the Thomas–Fermi profile (in Eq. (4)) is  $\kappa = \omega^2 \pi/g$  with  $g = \tilde{g}$  at very low temperature. The curvature increases (the profile becomes narrower) with  $T$  because particles spread out farther in the  $z$ -direction. Above the critical temperature, however, the curvature decreases (the profile becomes wider), as is natural for a thermal gas, with  $\kappa \propto n(0) \lambda^2$ . The curvature plot provides an intrinsic signature of the phase transition, at a temperature  $T/T_{\text{BEC}}^0 \simeq 0.70$ , which agrees nicely with the temperature at which the central density passes the critical value Eq. (2). We have also studied smaller systems (with  $N = 2250, 9000, 36\,000$ , and  $144\,000$ ) at unchanged values of  $T/T_{\text{BEC}}^0$  and  $\omega_z/T_{\text{BEC}}^0$ , but found only very small variations in the density profiles. Our value for the critical temperature,  $T_{\text{KT}} \simeq 0.70 T_{\text{BEC}}^0$  is close to the mean-field formula of Eq. (3), and somewhat higher than the experimental value [6]  $T_{\text{KT}}^{\text{exp}} \simeq 0.46(3) T_{\text{BEC}}^0$ .

The low-temperature phase below the Kosterlitz–Thouless transition is a superfluid. For a homogeneous system, the superfluid fraction can be probed through the response to boundary conditions, and easily computed within the path-integral formalism, through the winding-number formula [7]. Likewise, a trapped superfluid does not respond to an infinitely slow rotation of a trap leading to a non-classical moment of inertia,  $I_{\text{nc}}$ , which is smaller than the classical value  $I_{\text{cl}} = \int d\mathbf{r} r^2 n(r)$ . The non-classical moment of inertia can again be computed from the diagonal elements of the density matrix [15]. In a homogeneous system, the ratio of the non-classical mo-

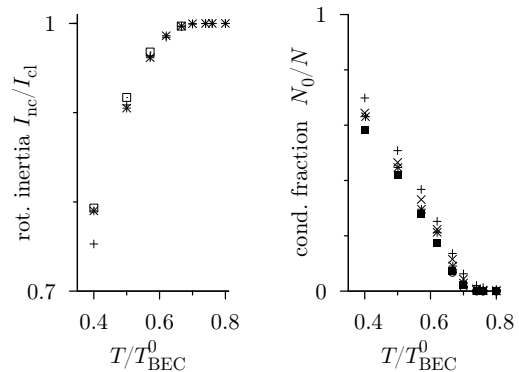


FIG. 4: *Left*: Non-classical moment of inertia  $I_{\text{nc}}/I_{\text{cl}}$  vs.  $T/T_{\text{BEC}}^0$  for  $N = 9000$  (crosses) and  $N = 144\,000$  (stars) compared to the ansatz of Eq. (5) (squares). *Right*: Condensate fraction for particle numbers ranging from  $N = 2250$  (crosses) to  $N = 144\,000$  (squares).

ment to the classical moment equals the normal fraction. In Fig. 4, we show that a superfluid phase emerges below  $T \simeq 0.70 T_{\text{BEC}}^0$ , and that  $I_{\text{nc}}/I_{\text{cl}}$  remains different from unity, independent on system size.

To interpret our data for the non-classical moment of inertia, we observe that in an infinite homogeneous system, at the Kosterlitz–Thouless transition, the superfluid density develops a universal jump[16],  $\Delta\rho_s = 2mT_{\text{KT}}/\pi$ , and the superfluid mass and the moment of inertia are both discontinuous. In the trap, the spatial structure smears out these discontinuities [14], but in local-density approximation, as mentioned, the gas is critical at the critical radius  $r_c$ . Therefore, we expect a normal phase beyond  $r_c$ , and a superfluid for  $r < r_c$ , with a jump of the superfluid density taking place at this radius and the superfluid density vanishing for  $r > r_c$ . For our parameters, the superfluid fraction at the critical radius is  $\rho_s(r_c)/n(r_c) = 2mT/n(r_c)\pi \simeq 0.5$ . We can continue the superfluid density  $\rho_s(r)$  into the inner region by a Thomas–Fermi profile:

$$\rho_s(r) = \begin{cases} m\omega^2 r_c^2 (1 - r^2/r_c^2)/2g + 2mT/\pi, & \text{for } r \leq r_c \\ 2mT/\pi & \text{for } r \rightarrow r_c^- \\ 0 & \text{for } r > r_c \end{cases} \quad (5)$$

(see Fig. 2). The non-classical moment of inertia  $I_{\text{nc}} = \int d\mathbf{r} r^2 [n(r) - \rho_s(r)]$ , computed using Eq. (5) and the computed density profile  $n(r)$ , agrees excellently with our data (see Fig. 4).

In the low-temperature phase of a two-dimensional superfluid, the condensate fraction vanishes in the thermodynamic limit. In a homogeneous system, the groundstate has zero momentum, and the fraction of particles occupying this state can be computed from the long-distance behavior of the non-diagonal one-body density matrix,  $\rho^{(1)}(\mathbf{r}, \mathbf{r}'; \beta)$  (see [7]). In an inhomogeneous system, the groundstate eigenfunction of the

one-body density matrix is no longer completely determined by symmetry. Still, in the rotationally symmetric trap the one-body density matrix is block-diagonal with respect to the Fourier components  $l$  of the angle between  $\mathbf{r}$  and  $\mathbf{r}'$ . Projection onto the Fourier components yields one-dimensional matrices,  $\rho_l^{(1)}(r, r'; \beta)$ , which can be discretized more easily than the bigger matrix  $\rho^{(1)}(\mathbf{r}, \mathbf{r}'; \beta)$ . The condensate fraction,  $N_0/N$ , corresponds to the largest eigenvalue with  $l = 0$ . Condensate wavefunctions computed this way for the three-dimensional trapped Bose gas, with Legendre polynomials replacing the Fourier components, closely agree with the solution of the three-dimensional Gross-Pitaevskii equation (see [17]). Figure 4 shows that the condensate fraction of our quasi two-dimensional system is rather large, but it decays algebraically with system size:  $N_0/N \sim N^{-\eta(T)/2}$ . The exponent  $\eta(T)$  depends on the temperature; we obtain  $\eta(0.70 T_{\text{BEC}}^0) \approx 0.5$  and  $\eta(0.67 T_{\text{BEC}}^0) \approx 0.2$ . Precisely at the critical temperature, we expect  $\eta(T_{\text{KT}}) \simeq 1/4$  which implies that the critical temperature is between  $0.67 T_{\text{BEC}}^0$  and  $0.70 T_{\text{BEC}}^0$ , comparable with our previous estimate,  $T_{\text{KT}} \simeq 0.70 T_{\text{BEC}}^0$ , based on the occurrence of a non-classical moment of inertia.

Our results are in qualitative agreement with recent experiments [6]. However, they found a lower critical temperature  $T_{\text{KT}}^{\text{exp}} = 0.46(3) T_{\text{BEC}}^0$ , and an almost Gaussian shape of the density profile above  $T_{\text{KT}}$ . In the specific experiment, the presence of several planes in the optical lattice renders the estimation of the critical temperature and the particle numbers difficult. More generally, we see from Fig. 1, even in the normal state away from  $T_{\text{KT}}$ , that the density profile deviates from the classical Gaussian distribution as soon as  $n(r)\lambda^2 \gtrsim 1$ . Therefore, only a small part of the density distribution can be used to gauge the temperature close to  $T_{\text{KT}}$ . Fitting a larger part of the distribution to a Gaussian typically yields a smaller width than the classical thermal distribution and therefore underestimates the true temperature of the system. This problem is even more pronounced when one analyzes column densities rather than radial profiles.

Notably, in the trap, the universal jump in the superfluid density of a two-dimensional superfluid at the critical temperature does not induce a significant discontinuity in the inertial response, as in two-dimensional films [18]. Nevertheless, the universal jump determines  $\rho_s(r)$  at the radius  $r = r_c$  where the gas is locally critical. Based on the local-density approximation, we proposed a superfluid density profile, Eq. (5), which continues the  $\rho_s(r)$  from  $r = r_c$  into the superfluid inner region. It depends on a single parameter  $r_c$  whose value can be determined directly from the density profile. The non-classical moment of inertia calculated from the superfluid density profile, Eq. (5), is in excellent agreement with a direct computation of this quantity. Further, it is re-

markable that in the finite Kosterlitz–Thouless system, the condensate fraction, which must vanish for an infinite system, is still rather large, even close to the transition temperature. The fact that the groundstate wavefunction of size  $\sim r_c$  remains macroscopically occupied for systems with particle number  $N \lesssim 10^6$  implies that the coherence of the atoms is neither destroyed by interparticle interactions nor by fluctuations, essential for building continuous and coherent sources of matter waves in lower dimensions [19].

We thank G. Baym, D. Ceperley, I. Cirac, J. Dalibard, and D. Guéry-Odelin for helpful discussions. M. H. acknowledges support from a CNRS-UIUC exchange grant.

- 
- [1] P. C. Hohenberg, *Phys. Rev.* **158**, 383 (1967).
  - [2] N. D. Mermin, *Phys. Rev.* **176**, 250 (1968); N. D. Mermin and H. Wagner, *Phys. Rev. Lett.* **22**, 1133 (1966).
  - [3] J. M. Kosterlitz and D. J. Thouless, *J. Phys. C* **6**, 1181 (1973); J. M. Kosterlitz, *J. Phys. C* **7**, 1046 (1974).
  - [4] V. L. Berezinskii, *Sov. Phys. JETP* **32**, 493 (1971); **34**, 610 (1972).
  - [5] Z. Hadzibabic, P. Krüger, M. Cheneau, B. Battelier, and J. Dalibard, *Nature* **441**, 1118 (2006).
  - [6] P. Krüger, Z. Hadzibabic, and J. Dalibard, *Phys. Rev. Lett.* **99**, 040402 (2007).
  - [7] E. L. Pollock and D. M. Ceperley, *Phys. Rev. B* **30**, 2555 (1984), *Phys. Rev. B* **36**, 8343 (1987); D. M. Ceperley, *Rev. Mod. Phys.* **67**, 1601 (1995).
  - [8] W. Krauth, *Phys. Rev. Lett.* **77**, 3695 (1996).
  - [9] M. Holzmann, W. Krauth, and M. Naraschewski, *Phys. Rev. A* **59**, 2956 (1999).
  - [10] M. Holzmann and Y. Castin, *Eur. Phys. J. D* **7**, 425 (1999).
  - [11] W. Krauth, *Statistical Mechanics: Algorithms and Computations*, Oxford University Press (Oxford, UK) (2006).
  - [12] V. Bagnato and D. Kleppner, *Phys. Rev. A* **44**, 7439 (1991).
  - [13] N. Prokof'ev, O. Ruebenacker, and B. Svistunov, *Phys. Rev. Lett.* **87**, 270402 (2001); N. Prokof'ev and B. Svistunov, *Phys. Rev. A* **66**, 043608 (2002); S. Sachdev and E. Demler, *Phys. Rev. B* **69**, 144504 (2004); S. Sachdev, *Phys. Rev. B* **59**, 14054 (1999).
  - [14] M. Holzmann, G. Baym, J.-P. Blaizot, and F. Lalœ, *Proc. Nat. Acad. Sci.* **104**, 1476 (2007).
  - [15] P. Sindzingre, M. L. Klein, and D. M. Ceperley, *Phys. Rev. Lett.* **63**, 1601 (1989).
  - [16] D. R. Nelson and J. M. Kosterlitz, *Phys. Rev. Lett.* **39**, 1201 (1977).
  - [17] M. Holzmann and W. Krauth (unpublished); M. Holzmann, thesis, Paris (2000) (unpublished).
  - [18] D. J. Bishop and J. D. Reppy, *Phys. Rev. Lett.* **40**, 1727 (1978); *Phys. Rev. B* **22**, 5171 (1980).
  - [19] P. Cren, C. F. Roos, A. Aclan, J. Dalibard, and D. Guéry-Odelin, *Eur. Phys. J. D* **20**, 107 (2002); T. Lahaye, J. M. Vogels, K. J. Günter, Z. Wang, J. Dalibard, and D. Guéry-Odelin, *Phys. Rev. Lett.* **93**, 093003 (2004).